

# Searching for links between magnetic fields and stellar evolution

## III. Measurement of magnetic fields in open cluster Ap stars with ESPaDOs <sup>★</sup>

J.D. Landstreet<sup>1</sup>, J. Silaj<sup>1</sup>, V. Andretta<sup>2</sup>, S. Bagnulo<sup>3</sup>, S.V. Berdyugina<sup>4,5</sup>, J.-F. Donati<sup>6</sup>, L. Fossati<sup>7</sup>, P. Petit<sup>6</sup>,  
J. Silvester<sup>8</sup>, and G.A. Wade<sup>8</sup>

<sup>1</sup> Physics & Astronomy Department, The University of Western Ontario, London, Ontario, Canada N6A 3K7.

e-mail: jlandstr@astro.uwo.ca, jsilaj@astro.uwo.ca

<sup>2</sup> INAF – Osservatorio Astronomico di Capodimonte, salita Moiariello 16, 80131 Napoli, Italy.

e-mail: andretta@na.astro.it

<sup>3</sup> Armagh Observatory, College Hill, Armagh BT61 9DG, Northern Ireland e-mail: sba@arm.ac.uk

<sup>4</sup> Institute of Astronomy, ETH, 8092 Zurich, Switzerland e-mail: sveta@astro.phys.ethz.ch

<sup>5</sup> Tuorla Observatory, University of Turku, FI-21500, Piikkiö, Finland

<sup>6</sup> Observatoire Midi-Pyrénées, 14, ave. Edouard-Belin, Toulouse, France e-mail: donati@ast.obs-mip.fr, petit@ast.obs-mip.fr

<sup>7</sup> Institut für Astronomie, Universität Wien, Türkenschanzstr. 17, A-1180 Wien, Austria e-mail: fossati@astro.univie.ac.at

<sup>8</sup> Department of Physics, Royal Military College of Canada, P.O. Box 17000, Station 'Forces', Kingston, Ontario, Canada K7K 7B4.  
e-mail: Gregg.Wade@rmc.ca

Received: September 15, 2009; accepted: ever hopeful

### ABSTRACT

**Context.** A small fraction of upper main sequence stars have strong, highly structured magnetic fields. The origin and evolution of these fields are not adequately understood.

**Aims.** We are carrying out a survey of magnetic fields in Ap stars in open clusters in order to obtain the first sample of magnetic upper main sequence stars with precisely known ages. These data will constrain theories of field evolution in these stars.

**Methods.** A survey of candidate open cluster magnetic Ap stars was carried out using the new ESPaDOs spectropolarimeter at the CFHT. This instrument provides an alternative to the FORS1 spectropolarimeter used up to now for this survey.

**Results.** We have obtained 44 measurements of the mean longitudinal fields ( $B_z$ ) of 23 B6 – A2 stars that have been identified as possible Ap stars and that are possible members of open clusters, with a median uncertainty of about 45 G. Of these stars, 10 have definite field detections. Nine stars of our sample are found not to be magnetic Ap stars. These observations significantly increase the information available about low-mass stars near the TAMS compared to our previous sample.

**Conclusions.** We find that ESPaDOs provides field measurements comparable to those that we have previously obtained with FORS1, and that these data also contain a large amount of useful information not readily obtained from lower resolution spectropolarimetry. With the new data we are able to expand the available data on low-mass, relatively evolved Ap stars, and identify more robustly which observed stars are actually magnetic Ap stars and cluster members. Re-analysis of the enlarged data set of cluster Ap stars indicates that such stars with masses in the range of 2 – 5  $M_\odot$  show RMS fields larger than about 1 kG only when they are near the ZAMS. The time scale on which these large fields disappear varies strongly with mass, ranging from about 250 Myr for stars of 2 – 3  $M_\odot$  to 15 Myr for stars of 4 – 5  $M_\odot$ . Our data are consistent either with emergent flux conservation for most (but not all) Ap stars, or with modest decline in flux with age.

**Key words.** Stars: magnetic fields – Stars: chemically peculiar – Stars: evolution – Polarization – Techniques: polarimetric

## 1. Introduction

The discovery that some A- and B-type stars of the upper main sequence possess strong (kG) magnetic fields was made more than 60 years ago (Babcock 1947). Since that time, there has been much investigation into the occurrence and structure of these fields, but much about them remains unknown. In particular, the evolution of these fields with time is a major area of ignorance, and until quite recently, almost no observational con-

straints have been available to guide and test theoretical ideas about field evolution.

In the past few years the observational situation has changed dramatically with the development of powerful new spectropolarimeters such as the one developed for the MuSiCoS spectrograph at the TBL, and FORS1 on the ESO VLT. With FORS1 one can obtain routine magnetic measurements of main sequence stars fainter than  $m_V \sim 10^m$ , and these new instruments have also made possible a general decrease in field measurement uncertainty by a factor of several.

The new generation of spectropolarimeters has for the first time made it practical to study observationally the evolution of magnetic fields in magnetic Ap stars with time, by exploring a large sample of such stars that are members of open clusters. Cluster studies open the possibility of obtaining a sample

Send offprint requests to: J. Landstreet

<sup>★</sup> Based on observations made with the Canada-France-Hawaii Telescope, operated by the National Research Council of Canada, the Centre National de Recherche Scientifique of France, and the University of Hawaii, under programme 05A-C19

of magnetic stars with reasonably accurate ages, thus providing a statistical time sequence of upper main sequence magnetism. Photometric and spectroscopic surveys have identified a substantial sample of probable Ap stars in such clusters which can be surveyed for fields with the new instruments, and the membership of these stars in their clusters can be established much more securely than in the past thanks to recent advances in astrometry, especially the Hipparcos and Tycho-2 projects.

These new possibilities have stimulated a major survey of magnetic fields in cluster Ap stars, whose first results have been reported by Bagnulo, Landstreet, Mason et al. (2006, hereafter Paper I) and analysed by Landstreet, Bagnulo, Andretta et al. (2007, hereafter Paper II). In the work completed so far, we have obtained and collected magnetic measurements of 81 stars which are both probable magnetic Ap stars and probable cluster members. The absolute (log) ages of the stars in this sample are known with accuracy in the range of 0.05 – 0.2 dex (the age uncertainty of the clusters themselves). The fraction of the main sequence lifetime elapsed (the “fractional age”) of each of the stars of this sample is known with a precision that is usually less than half the fractional age itself, and thus for stars of small fractional age, the fractional age is also quite precise.

From this sample, we have established conclusively that fields are present in Ap stars more massive than  $2M_{\odot}$  from the ZAMS onwards. We have also shown that stars more massive than about  $3M_{\odot}$  have a substantial decline in field strength after the age of about  $3 \times 10^7$  yr, while less massive stars show no strong evidence of change of field strength even as long as  $10^9$  yr after reaching the ZAMS.

Recently the powerful new spectropolarimeter ESPaDOnS has become available at the CFHT. This instrument combines a large resolving power with high throughput and wide spectral coverage, and is the most powerful instrument for field measurement in stars with reasonably rich spectra and low  $v_e \sin i$  that is currently available. We have used ESPaDOnS to extend the survey described and analysed in Papers I and II.

This extension of our previous survey has several aims: (1) to expand the survey into the northern celestial hemisphere, adding clusters not visible from ESO; (2) to increase the number of observations of stars for which only one or two magnetic measurements are available, thereby improving the precision of  $B_{rms}$  values available for stars of the survey; (3) to search for fields in probable magnetic Ap stars for which no fields have yet been detected by the available observations, exploiting the superior ability of ESPaDOnS to detect weak fields, and to detect fields even when the mean longitudinal field  $\langle B_z \rangle$  is close to zero (see discussion below); and (4) to compare the field measurement accuracy obtained with high- and low-resolution spectropolarimetry for various kinds of magnetic Ap stars.

The next section of this paper discusses the observational strategy employed, the data reductions, and the choice of stars to observe. Sect. 3 describes the transformation of the polarisation measurements into measurements of  $\langle B_z \rangle$ , and tests of the data quality. Sect. 4 presents the new field measurements obtained. In this section we also compare the observational efficiencies of various instruments. Sect. 5 contains a star-by-star assessment of the new information obtained from the ESPaDOnS observations. In Sect. 6 we discuss general features of the new addition to our data set of cluster magnetic Ap stars. In Sect. 7 the new cluster field measurements are integrated into our larger survey, and the conclusions of Paper II are reviewed in the light of our new data. Finally Sect. 8 summarises the conclusions of the paper.

## 2. Instrumentation, observations and data reduction

### 2.1. ESPaDOnS

The instrument used for this portion of our survey of magnetic Ap stars in clusters is ESPaDOnS, the new cross-dispersed echelle spectropolarimeter built for the Canada-France-Hawaii telescope. The instrument is conceptually similar to the MuSiCoS spectropolarimeter which has been extensively used for high-precision magnetic measurements (e.g. Wade et al. 2000a, 2000b), but has a factor of about 30 times higher efficiency.

The polarisation analyser is located at the Cassegrain focus of the telescope. The stellar image is formed on an aperture followed by a collimating lens. The beam then passes through a rotatable  $\lambda/2$  waveplate, a fixed  $\lambda/4$  waveplate, a second rotatable  $\lambda/2$  waveplate, and finally a small-angle Wollaston prism, followed by a lens which refocuses the (now double) star image on the input of two optical fibres. This relatively complex polarisation analyser is necessary because one of the fundamental design parameters for ESPaDOnS was very wide wavelength coverage (approximately 3700 Å to 1.04  $\mu\text{m}$ ). To have waveplates which are approximately achromatic over this wide range, ESPaDOnS uses Fresnel rhombs. A single Fresnel rhomb acts as a  $\lambda/4$  plate, but deviates the beam, while two Fresnel rhombs in series form a  $\lambda/2$  plate without beam deviation. To minimise mechanical complications, only the double (non-deviating) Fresnel rhombs are allowed to rotate; the configuration chosen is the minimum which allows one to analyse all of the Stokes polarisation components ( $Q, U, V$ ) by appropriate orientation of the axes of the successive waveplates.

The two output beams from the Wollaston prism, which have been analysed into the two components of linear or circular polarisation as desired by appropriate waveplate settings, are then carried by the pair of optical fibres to a stationary and thermally buffered (but not yet temperature-controlled) cross-dispersed spectrograph where two interleaved spectra are formed, covering virtually the entire desired wavelength range with a resolving power of  $R \approx 65\,000$ . The  $I$  component of the stellar Stokes vector is formed by adding the two corresponding spectra, while the desired polarisation component ( $Q, U, V$ ) is obtained essentially from the difference of the two spectra. To minimise the systematic errors due to small misalignments, differences in transmission, effects of seeing, etc., one complete polarisation observation of a star consists of four successive spectra taken with four different positions of the two rotatable Fresnel rhombs; for the second and third exposures, the waveplate settings exchange the right and left circularly analysed beams with respect to the handedness measured in the first and fourth exposures (cf. Donati et al. 1997; Donati et al. in preparation; <http://www.cfht.hawaii.edu/Instruments/Spectroscopy/Espadons/>).

### 2.2. Observations

The stars observed were selected from a large data-base we have assembled (see Papers I and II) of possible magnetic Ap stars that are also possible members of open clusters within about 1 kpc of the Sun. As discussed in Paper II, we have used available astrometric and photometric data, especially those from the Hipparcos (ESA 1997) and Tycho-2 (Høg et al. 2000a, 2000b) catalogues, to clarify as far as possible which magnetic Ap stars are probable or definite cluster members. Here we use essentially the same criteria for cluster membership that were discussed in

Paper II. We selected stars from the data-base that were observable in July 2005, when these observations were carried out. In part, we observed stars that are not observable from ESO, where we have obtained the previous observations for this survey. However, a number of observations were obtained of stars for which previous measurements are available, either by us or by others.

As discussed in detail in Paper II, the classification of most of the stars observed as magnetic Ap stars is still fairly uncertain, because identification of cluster Ap stars is usually based only on narrow-band photometry and/or low dispersion, low signal-to-noise spectra. Thus we expected that some of the stars observed would turn out not to be magnetic Ap stars at all.

Our previous observations for this survey were carried out using the low-resolution spectropolarimeter FORS1 at the ESO VLT. With  $R \sim 10^3$ , FORS1 magnetic field measurements give high weight to the circular polarisation signal in the Balmer lines, which are resolved even at this low dispersion. In cases where a relatively rich metallic spectrum is present, the FORS1 measurements can be made significantly more precise by exploiting the polarisation signal present in the (barely resolved) metallic line spectrum, but to first order the precision of FORS1 magnetic field measurements is not sensitive to the details of the metallic line spectrum. In contrast, measurements with ESPaDOnS, like those obtained with MuSiCoS, have high enough resolving power to fully exploit the information content of the metallic line spectrum. ESPaDOnS field measurements have standard errors which decrease strongly with decreasing  $v_e \sin i$  and with increasing richness and strength of the metallic line spectrum (cf. Landstreet 1982; Shorlin et al. 2002). To fully exploit this dependence, and thus to obtain the most precise measurements possible, we have preferentially observed relatively cool magnetic Ap stars, and have selected our targets for low  $v_e \sin i$  where available data allowed us to select targets with this criterion.

The list of stars observed is given in Table 1, which contains the name of each star, the cluster to which it may belong, our assessment of the probability that the star is actually a cluster member (Y = definite member, P = probable member, ? = questionable, assessed as in Paper II), the spectral type based on a combination of published types with the results of our own examination of individual  $I$  spectra, and the  $v_e \sin i$  value deduced from our ESPaDOnS spectra (the uncertainty in these values is approximately the larger of  $\pm 10\%$  or  $\pm 2 \text{ km s}^{-1}$ ).

### 2.3. Data Reduction

The observed polarised spectra were reduced to 1D using the dedicated software LibreEsprit, provided by J.-F. Donati for treatment of ESPaDOnS data. LibreEsprit subtracts bias, locates the various spectral orders on the CCD image, measures the shape of each order and models the (varying) slit geometry, identifies comparison lines for each order and computes a global wavelength model of all orders, performs an optimal extraction of each order, and combines the resulting spectra (in groups of four, corresponding to the four sub-observations with the four different Fresnel rhomb settings) to obtain intensity ( $I$ ) and circular polarisation ( $V$ ) spectra. The  $V$  spectrum normally has the continuum polarisation removed, as this arises mainly from instrumental effects and carries little information about the star. Each spectrum is corrected to the heliocentric frame of reference, and may optionally be divided by a flat field and be approximately normalised (see Donati et al. 1997, and Web pages at <http://www.cfht.hawaii.edu/Instruments/Spectroscopy/Espadons>).

**Table 1.** Stars observed with ESPaDOnS for magnetic fields

Star	Cluster	Memb	Spectrum	$v \sin i$ ( $\text{km s}^{-1}$ )
HD 16605	NGC 1039	P	A1p SiCrSr	18
HD 16728	NGC 1039	Y	B9V	75
HD 19805	$\alpha$ Per	Y	B9.5V	8
HD 108945	Coma Ber	Y	A2p SrCr	65
HD 144661	Upper Sco	Y	B8p He-wk	45
HD 153948	NGC 6281	P	Ap Si	80
HD 317857	NGC 6383	?	A1IVp	26
HD 318100	NGC 6405	Y	B9p	42
HD 320764	NGC 6475	P	A1V an	225
HD 162576	NGC 6475	Y	B9.5p SiCr	30
HD 162588	NGC 6475	Y	Ap Cr	73
HD 162630	NGC 6475	P	B9V	51
HD 162656	NGC 6475	Y	B9V	45
HD 162725	NGC 6475	Y	A0p SiCr	32
HD 169842	NGC 6633	Y	A1p SrCr	45
HD 169959A	NGC 6633	?	A0p Si	57
HD 170054	NGC 6633	Y	B6IV	26
HD 170860	IC 4725	P	B9IV/Vp	85
HD 172271	IC 4756	P	A0p Cr	107
HD 205073	NGC 7092	Y	A1	16
HD 205331	NGC 7092	Y	A1V	51
BD+49 3789	NGC 7243	P	B7p Si	81
HIP 109911	NGC 7243	Y	A0Vp Si	59

A check spectrum called the  $N$  spectrum, computed by combining the four observations of polarisation in such a way as to have real polarisation cancel out, is also calculated by LibreEsprit. The  $N$  spectrum tests the system for spurious polarisation signals. In all of our observations, the  $N$  spectrum is quite featureless, as expected.

The final spectra consist of ASCII files tabulating  $I$ ,  $V$ ,  $N$ , and estimated uncertainty per pixel as a function of wavelength, order by order. We have kept both normalised and un-normalised versions of each spectrum.

### 3. Measurement of magnetic field strength

Two methods allow us to detect magnetic fields in the stars observed. First, we can use the  $V$  spectra to measure the mean longitudinal magnetic field strength  $\langle B_z \rangle$  of each star at the time of observation. This is the conventional measure of field strength normally used for detection of fields in magnetic Ap stars (e.g. Landstreet 1982). However, because of the high value of resolving power, we can also examine spectral lines for the presence of circular polarisation signatures; Zeeman splitting combined with Doppler broadening of lines by rotation can lead to non-zero values of  $V$  within spectral lines even when the value of  $\langle B_z \rangle$  is close to zero. This possibility substantially increases the sensitivity of our measurements as a discriminant of whether a star is in fact a magnetic star or not, as discussed by Wade et al. (2000a) and Shorlin et al. (2002).

Because ESPaDOnS is a high-resolution instrument and because the stars observed are relatively faint (typical magnitudes  $m_V$  between 6 and 10), the signal-to-noise ratio (SNR) in individual spectral lines is not very high, and field measurements made with single lines are not very precise. In this situation, we employed the technique of Least Squares Deconvolution (LSD), developed into a practical strategy by Donati et al. (1997) and employed extensively in the analysis of magnetic observa-

tions made with the MuSiCoS spectropolarimeter (cf Wade et al. 2000a).

In the LSD technique, we start with a list of spectral lines expected in a normal or a magnetic Ap star of a temperature near that of the star observed. This line list is obtained from the Vienna Atomic Line Database (VALD; Piskunov et al. 1995; Ryabchikova et al. 1999; Kupka et al. 1999), and is selected by specifying a suitable chemical composition, wavelength range, and minimum line depth. For the stars in our sample, two different abundance tables were employed. An Ap abundance table was created by assigning the iron-peak elements abundances  $10\times$  solar abundance, except for chromium which was increased to  $100\times$  solar. A solar abundance table is the default provided by VALD when a request is made, and was used to make the remaining lists. VALD line lists were requested to include all lines in the ESPaDOnS spectral range (3700–10000 Å) with depths greater than 10% of the continuum (in a synthetic spectrum with  $v_e \sin i = 0$ ).

Fundamental parameters (effective temperature  $T_{\text{eff}}$  and surface gravity) for the stars observed were determined primarily from Strömgren and/or Geneva photometry, as described in detail in Paper II. Neither Strömgren photometry nor Geneva photometry is available for the stars HD 169842, HD 172271 and HD 317857, so the effective temperatures were estimated from Johnson UB<sub>V</sub> photometry or the observed spectra. Initial selection of an appropriate LSD line list for each star was made based on these values. Experimentation showed that the highest SNR in the measured field  $\langle B_z \rangle$  generally resulted from the use of a line list selected with a temperature close to, or up to about 10–15% hotter than, the estimated  $T_{\text{eff}}$  of the star. (Using a line list appropriate for a slightly hotter star seems to eliminate a number of weak lines that contribute more to the noise than to the signal.)

For each spectral line in the line list appropriate to a particular star, a small window is cut out of the observed  $I$  and  $V$  spectra centred on the laboratory wavelength of the line, and the local wavelength scale is converted to a velocity scale relative to the nominal central wavelength. Conceptually, one may imagine that all the small  $I$  and  $V$  spectral windows are then averaged. (In practice, model intensity and polarisation signatures are fit to the ensemble of single line data windows, rather than performing direct averaging.) In this average, each window is given a weight proportional to the line depth, the wavelength, and the Landé factor of the line. Since the  $I$  and  $V$  signatures in individual spectral lines are very similar to one another, and scale essentially with the weighting factors used in averaging, the resulting mean intensity and polarisation line profiles may be analysed as if they represented a single real spectral line having a much higher SNR than the individual observed lines. The improvement in SNR from single lines to the LSD line is by roughly the square root of the number of lines used, so the SNR in the LSD mean line is typically of order 30 times higher than in single lines.

The LSD line is then analysed in two ways. First, the value of  $\langle B_z \rangle$  is computed using the normal expression (e.g. Donati et al. 1997)

$$\langle B_z \rangle = -2.14 \cdot 10^{12} \frac{\int v V(v) dv}{\lambda z c \int [I_c - I(v)] dv}, \quad (1)$$

where  $\langle B_z \rangle$  is in G,  $z$  is the mean Landé factor of the LSD line (typically about 1.25), and  $\lambda$  is the weighted mean wavelength of the LSD line in Å (typically about 5200 Å). The limits of integration were chosen visually for each star to coincide with the apparent edges of the LSD  $I$  and  $V$  lines; using a smaller window

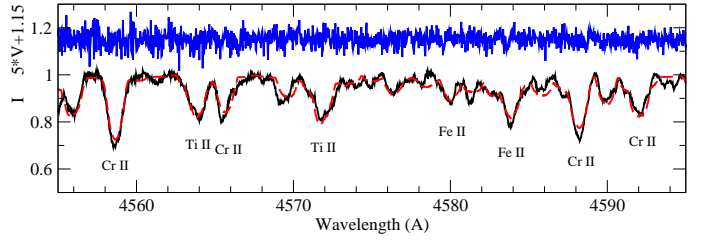


**Fig. 1.** A sample region of the  $I$  spectrum of HD 169842 with identification of strong lines (lower solid line) is compared to a synthetic spectrum (dashed line), for which Cr has been enhanced by a factor of about 80. Above is the same region of the  $V$  spectrum, multiplied by 5 and displaced upward by 1.15 for clarity.

would neglect some of the signal coming from the limb of the star, while a window larger than the actual line would increase the noise without adding any further signal, thus degrading the SNR below the optimum value achievable. If the resulting value of  $\langle B_z \rangle$  is significantly non-zero (say by  $4 - 5\sigma_B$  in a single observation, or by  $3\sigma_B$  in two or more observations), we conclude that a magnetic field has been detected.

In addition, the LSD line profile itself is examined. If the value of  $V$  rises to a statistically significant value inside the line, while always remaining insignificant in the neighboring continuum, we conclude that a field is detected. As mentioned above, this may occur even if  $\langle B_z \rangle$  is not significantly different from zero. On the other hand, from our experience with searches for weak fields in known Ap stars (cf Aurière et al. 2007), a star with a favourable spectrum (hundreds of lines and  $v_e \sin i$  less than about 50 or 60 km s<sup>-1</sup>) which shows no significantly non-zero values of  $V$  within the LSD spectral line in two independent high SNR observations is unlikely to host a magnetic field. Furthermore, since observations with ESPaDOnS yield high-resolution  $I$  spectra (as well as  $V$  spectra), we may test the suspicion that a star is in fact not a magnetic Ap star at all by examining the  $I$  spectrum. The combination of no significant  $V$  signature with a normal  $I$  spectrum has confirmed that several of the stars selected for observation are indeed not Ap stars.

As an example, small segments of the ESPaDOnS  $I$  and  $V$  spectra of HD 169842 from JD 2453566.902 are shown in Figure 1. The  $I$  spectrum is compared to a synthetic spectrum computed using the magnetic line synthesis programme Zeeman (cf. Landstreet 1988) with (nearly) solar abundances except for Cr, which is enhanced by 1.9 dex. Note that no trace of Zeeman polarisation is seen in individual spectral lines; in this star the Zeeman signal is too small relative to the noise level in  $V$  to be directly visible. The LSD  $I$  and  $V$  spectra computed from these data are shown in Figure 2. Averaging over 4836 spectral lines has reduced the noise in the LSD  $V$  spectrum by a factor of order 30 relative to the noise level in individual spectral lines, allowing the magnetic field signature in  $V$  to be clearly seen with an amplitude well above the small noise level outside the line. (The number of lines used in the LSD mask is a strong function of both  $T_{\text{eff}}$  and degree of peculiarity. The Ap masks used have about 8300 lines for a star of  $T_{\text{eff}} \sim 8500$  K, decreasing smoothly to about 1600 lines at  $T_{\text{eff}} \sim 15000$  K. Typically the masks for normal composition have about 1/3 as many lines as the Ap masks.)

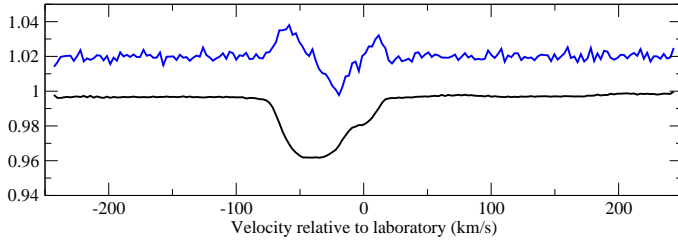


**Fig. 2.** The LSD  $I$  (lower) and  $V$  (upper; multiplied by 25 and displaced upwards by 1.02 for visibility) spectra of HD 169842 from the same night as Figure 1.

### 3.1. Verification

One important kind of verification of the performance of ESPaDOnS is to confirm that it does not produce spurious magnetic field detections. We have tested this in two ways. First, we have made a precise field measurement ( $-9 \pm 19$  G) of the apparently non-magnetic star  $\alpha$  And (= HD 358), which, in agreement with numerous other measurements made with a variety of instruments, shows no significant field (Wade et al. 2006). Secondly, we find in the present data a number of stars which turn out (on the basis of our new high-resolution  $I$  spectra) to be normal rather than magnetic Ap stars; invariably such stars also do not show any significant magnetic field.

We have also verified that our field measurements are consistent with earlier work by observing the longitudinal field of the well-studied magnetic Ap star  $\alpha^2$  CVn during three nights. These data are presented in Table 2. We have computed phases (at the mid-point of each observation) according to the ephemeris of Wade et al. (2000b), and we compare the three new measurements with their magnetic curve in Figure 3. It is clear from the figure that the new observations are fully consistent with the previous (MuSiCoS) data obtained and reduced in a very similar way, but the ESPaDOnS data are about a factor of five more precise.

**Table 2.** Observations of standard star  $\alpha^2$  CVn

HJD	SNR	phase	$\langle B_z \rangle \pm \sigma_B$ (G)
2453569.748	680	$0.570 \pm 0.01$	$589 \pm 11$
2453570.747	1040	$0.752 \pm 0.01$	$-619 \pm 10$
2453571.738	580	$0.934 \pm 0.01$	$-739 \pm 11$

## 4. Results

The field measurements obtained during the ESPaDOnS survey are presented in Table 3. This table lists the stars for which field measurement was successful; the heliocentric Julian date (HJD) of each observation; the signal-to-noise ratio (SNR) achieved per Å of spectrum, derived from the value reported in the output file of LibreSprit for the  $N$  spectrum of order 45 at 5030 Å; the measured value of the stellar heliocentric radial velocity  $v_r$  (in  $\text{km s}^{-1}$ ; generally accurate to about  $\pm 1 - 2 \text{ km s}^{-1}$ ); the measured mean longitudinal field strength  $\langle B_z \rangle$  (in G) with its standard error (computed by treating each integration pixel as independent, using the uncertainty per pixel of  $V$  assigned by the LSD process); and finally a flag (fld) that indicates whether a field has

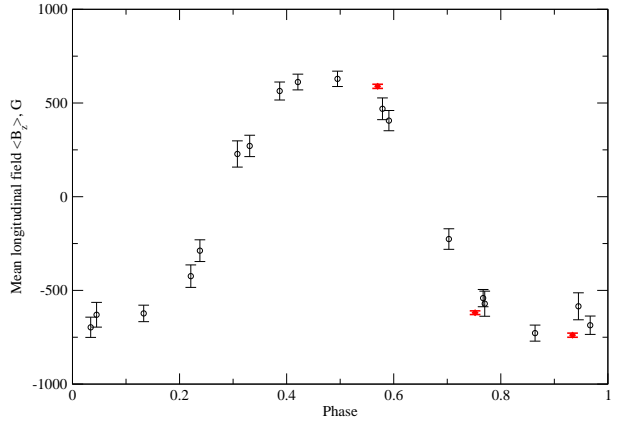


**Fig. 3.** Phased magnetic mean longitudinal field variations of  $\alpha^2$  CVn as reported by Wade et al. 2000b (open circles). Our three new data points (filled circles) are those with very small error bars.

been definitely detected (DD) or not (blank). Note that the radial velocity has been measured from the LSD spectrum by bisecting the line wings close to where they reach the continuum. The precision of such a measurement is limited primarily by the width and shallowness of the line profile and occasionally by the unusual shape; the absolute precision of ESPaDOnS radial velocities for very sharp-line stars is a few hundred  $\text{m s}^{-1}$ , and the stability is on the order of a few tens of  $\text{m s}^{-1}$ .

As discussed above, a field may be detected through the  $V$  signature even if  $\langle B_z \rangle$  is close to zero, as is the case for example of one observation each of HD 108945, HD 162576 and HD 162725. On the other hand, the field of a star which is actually a magnetic Ap star may not be detected, for example if the field is particularly weak (of order 100 G or less), if the spectrum is strongly broadened by rotation, if  $T_{\text{eff}}$  is high and there are relatively few metal lines, or if the SNR of the spectrum obtained is too low.

It is of interest to compare the relative measurement efficiencies of magnetic measurements made with low and high spectral resolution. We can obtain such a comparison by examining measurements of the same star made with FORS1 and ESPaDOnS. Fortunately we have in our data sets several stars observed with both instruments.

In Table 4 we compare measurements of the same star made with FORS1 and with ESPaDOnS. This table lists individual stars, magnitude  $m_V$ , the important parameters  $T_{\text{eff}}$  (determined as in Paper II) and  $v_e \sin i$  which have a strong influence on the precision of ESPaDOnS measurements, and then for specific measurements with FORS1 or ESPaDOnS we list HJD of observation, the total time required for an observation (including telescope setting time)  $\Delta t$ , the resulting field measurement with its uncertainty, and whether a field was detected (for FORS1, as in Paper I, nnn means no detection, DnD means definite detection only in Balmer lines, and DDD means detection in both Balmer lines and the metal spectrum; for ESPaDOnS measurements, ND means no detection, DD means definite detection).

Note that overheads for a single magnetic field measurement with FORS1 total about 20 min (in “fast” mode). For stars brighter than  $m_V = 8$  or 9, the integration time is small compared to the overheads, so the time-on-target for such bright stars will be independent of magnitude. (The justification for using FORS1 in this inefficient mode was its uniqueness in the southern hemisphere. FORS1 showed its full capabilities in the de-



tection of a field in a broad-lined Ap star of  $m_V = 12.9$ ; see Bagnulo et al. 2004.) The overheads for a full ESPaDOnS magnetic measurement total about 9 min, so the time-on-target for ESPaDOnS exposures is dominated by the actual exposure time for stars fainter than about  $m_V = 6$ .

In examining Table 4, it is worth recalling that because low-resolution spectropolarimetry, such as the FORS1 measurements, relies heavily on the polarisation in the wings of the Balmer lines, which do not vary greatly over the spectral range of our survey, the measurement uncertainties obtained using this class of techniques tend to fall within a moderate range. Inspection of Table A.3 of Paper I shows that most of the measurements there have standard errors between about 40 and 90 G, while the most accurate measurements have  $\sigma_B \approx 30$  G. This is also true of the subset of data in Table 4, where all the uncertainties are in the range of 33 – 77 G. In contrast, the uncertainties of high-resolution spectropolarimetry, such as the ESPaDOnS data, are significantly more scattered. The precision of a high-resolution Zeeman measurement depends strongly on the number and strength of spectral lines, on  $v_e \sin i$ , and on the total signal collected. Very precise measurements ( $\sigma_B$  as low as a few G) are possible for stars having many sharp and deep lines (compare Wade et al. 2006). More than 1/3 of the ESPaDOnS measurements have  $\sigma_B \leq 30$  G, while about 20% of our observations have  $\sigma_B > 100$  G; the largest  $\sigma_B$ s in Table 3 are over 400 G.

Examination of Table 4 reveals that in similar  $\Delta t$ s, ESPaDOnS and FORS1 often obtain measurements with roughly similar field strength uncertainties. The ESPaDOnS measurements are substantially less precise primarily for stars with values of  $v_e \sin i$  above 60 or 70 km s<sup>-1</sup> (HD 153948), for stars with  $T_{\text{eff}}$  above perhaps 12 000 K (HD 170054), or for stars for which insufficient signal was obtained due to faintness, weather or other conditions. On the other hand, in cases of particularly favourable circumstances (cool stars with low  $v_e \sin i$ ), the  $\sigma_B$ s can be very low, even below 20 G (HD 19805, HD 162725, HD 205073).

The reason that an instrument such as ESPaDOnS, on a 3.6-m telescope, can be competitive with one on an 8-m telescope is partly a consequence of the way in which the high-resolution instrument can exploit more fully the information content of the metallic-line spectrum of the star observed. However, other factors are also involved. In the particular case of FORS1, observations of bright stars ( $m_V < 10$ ) have a very low duty cycle. Most of the observing time is spent setting on target and closing the loop on the adaptive optics, and on reading out the CCD. The actual shutter time on such a star is only a few minutes out of the roughly 30 min needed for a typical bright star observation. For stars fainter than 10<sup>m</sup>, for which longer integration times are required (e.g. 2 hr for the  $m_V \approx 13^m$  star NGC 2244-334; Bagnulo et al. 2004), the instrument on the larger telescope achieves a much higher duty cycle, and the aperture advantage is much more important.

## 5. Individual stars

Because each ESPaDOnS observation provides not only a magnetic measurement but also a high-dispersion spectrum covering some 7000 Å through the visible and near-IR, these data can provide a number of useful pieces of information. We obtain a measurement of the mean longitudinal field as well as supplementary information about the presence or absence of a magnetic field from the behaviour of  $V$  within the LSD  $I$  line profile. We can also measure the projected rotation velocity  $v_e \sin i$ , and

the stellar radial velocity  $v_r$ . The value of  $v_e \sin i$  provides a constraint on possible rotation periods, and  $v_r$  provides a potentially useful test of cluster membership. We can use the shape of the LSD  $I$  profile, and its possible variations if we have multiple observations, as valuable additional clues to test whether a doubtful star is actually a magnetic Ap star. Finally, we can examine (and even model) the observed  $I$  spectrum to characterise the chemical composition of the atmosphere in order to securely establish peculiarity or normality. In this section we discuss the information obtained about each of the stars studied.

### 5.1. HD 16605 = NGC 1039-154, A1p SiSrCr

The large field of this star was first reported by Kudryavtsev et al. (2006). Our two measurements confirm their result. All five available measurements show negative fields, ranging from -840 to -2430 G. The observed  $v_e \sin i = 18$  km s<sup>-1</sup> (see Table 1) suggests a rotation period of a few days. The star is certainly a magnetic Ap star.

Proper motion data (see Paper II) for this star indicate probable membership in NGC 1039, as does the star's position near the cluster isochrone in the HR Diagram. The radial velocity measured for this star is about -1 km s<sup>-1</sup>. Our two observations show no variation of this quantity, and the three spectra obtained by Kudryavtsev et al. (2006) yield  $v_r$  values that are consistent with our measurements (Kudryavtsev, private communication). Thus it appears that this star is probably not a spectroscopic binary. However, the radial velocity of the cluster is reported by Kharchenko et al. (2005) to be  $-15 \pm 2.3$  km s<sup>-1</sup>. Furthermore, nearly 50 radial velocities have been measured in low-mass main sequence stars in this cluster by Jones et al. (1997); omitting two stars with strongly discordant radial velocities, the median cluster velocity is about -10 km s<sup>-1</sup> with a dispersion of approximately 4 km s<sup>-1</sup>. It is not clear what the origin of the discrepancy between these two cluster radial velocities is, but since the Jones et al. data are published, we adopt the median of their values as the cluster mean  $v_r$ . Thus the radial velocity of HD 16605 is about  $2\sigma$  from the cluster median. This discordant radial velocity is possibly an indication of non-membership in NGC 1039, but with all other indicators of membership in favour of membership, we still regard HD 16605 as a probable cluster member.

### 5.2. HD 16728 = NGC 1039-307, B9V

No previous magnetic observations of this star are available in the literature. We have two observations of the star. One has very low SNR for a reason that we have not been able to determine, and is omitted from Table 3. The second measurement yields a  $\langle B_z \rangle$  value with an uncertainty of almost 300 G, mainly because the LSD spectral line is shallow and broad, with a  $v_e \sin i$  of about 75 km s<sup>-1</sup>. The line profile shape could be that of an SB2. Synthesis of a small section of the ESPaDOnS  $I$  spectrum indicates that the atmospheric abundances in this star are close to solar values. (Systematic synthesis of ESPaDOnS  $I$  spectra will be a separate aspect of the investigation of these data which will be reported in a later paper. Here we simply provide a few first results that help us to separate magnetic Ap stars from other classes of stars.) It appears that this star is probably a normal star of  $T_{\text{eff}} \approx 11500$  K rather than a magnetic Ap star.

Proper motion data indicate that this star is probably a member of NGC 1039 (Baumgardt et al. 2000; Dias et al. 2001). Because it is not clear from our observations whether the star is single or is a spectroscopic binary, we cannot test cluster mem-

bership with a  $v_r$  measurement. We consider HD 16728 to be a probable cluster member.

### 5.3. HD 19805 = Melotte 20-167, B9.5V

A large magnetic field of order 1 kG was reported by Bychkov et al. (2003), based on four unpublished measurements. However, three unpublished observations of the star using MuSiCoS, with  $\sigma_{BS}$  in the range of 125 – 175 G, do not reveal any sign of such a large field. Our two observations, with uncertainties for  $\langle B_z \rangle$  of 24 and 14 G, also show no indication of any field, nor is a significant Zeeman effect detected in  $V$ . In addition, the spectrum of this star closely resembles that of a normal star of  $T_{\text{eff}} \approx 10200$  K, with strong He I and O I, normal Cr II, and no obvious sign of rare earths. Synthesis of  $I$  in small spectral regions confirms essentially solar abundances of these elements. We classify this star as normal.

On the basis of proper motions, this star is a member of the  $\alpha$  Per cluster, Melotte 20 (de Zeeuw et al. 1999). Robichon et al. (1999) give the cluster velocity as  $-0.2 \pm 0.5$  km s $^{-1}$ ; the values tabulated by Kharchenko et al. (2005) are similar. Our observed radial velocity  $v_r = 0$  km s $^{-1}$  is consistent with membership; we consider this star to be a cluster member.

### 5.4. HD 108945 = Melotte 111-160, A2p SrCr

A weak field ( $109 \pm 44$  G) was definitely detected in this star by Shorlin et al. (2002). One measurement using FORS1 was reported in Kochukhov & Bagnulo (2006), where the field value is based only on the Balmer lines; no field was detected. In Table 4 we give the field value measured from these same ESO archival spectra using both Balmer and metal lines; again no field is detected, with  $\sigma_B = 75$  G. In two of our three ESPaDOnS measurements,  $\langle B_z \rangle$  is non-zero at more than the  $3\sigma_B$  level, although the field is always of order 100 G or less. Furthermore, in all three measurements, a clearly non-zero signal is found in  $V$ , confirming the reality of the small fields measured. HD 108945 is certainly a magnetic Ap star.

Proper motion data (cf Paper II) indicate that this star is a member of the Coma Berenices cluster. The mean cluster  $v_r$  is  $-0.1 \pm 0.2$  km s $^{-1}$  (Robichon et al. 1999). Our measured radial velocity of  $+1$  km s $^{-1}$  is consistent with membership; we consider this star a cluster member.

### 5.5. HD 144661 = HIP 79031, B8p He-wk

Three  $\langle B_z \rangle$  observations of this He-weak star, with  $\sigma_B \sim 200$  G, were made by Borra et al. (1983), but no strong evidence of a field was found. Our two magnetic measurements ( $\sigma_B \sim 50$  G) yield  $\langle B_z \rangle$  values not significantly different from zero, and no sign of a magnetic signature is found in either  $V$  line profile. The LSD line profile is constant and appears to be a simple rotational profile. Borra et al. reported that this star is a member of the PGa class of He-weak stars, which seems to be a high-temperature extension of the HgMn stars and, like the HgMn stars, seem to be chemically peculiar but non-magnetic. Woolf & Lambert (1999) suggest that the star is Hg-rich. Synthesis of a small section of spectrum shows that the atmosphere is depleted in He (by more than 1 dex) and S, almost normal in Si, and about 0.5 dex overabundant in Fe (see also Norris 1971). We classify HD 144661 as a non-magnetic, He-wk (probably PGa; cf Borra et al. 1983) star.

On the basis of proper motions (de Zeeuw et al. 1999) the star is a member of Sco OB2. de Zeeuw et al. give a mean radial velocity of  $-4.6$  km s $^{-1}$  for the Upper Sco region of the association. Our  $v_r$  values are consistent with this value, and we consider the star an association member.

### 5.6. HD 153948 = NGC 6281-15, Ap Si

A field of about 200 G was detected in this star using FORS1 (Paper I). All three of our measurements yield fields of about this size, although none of the  $\langle B_z \rangle$  values differs from zero by  $3\sigma_B$ . However, two of our observations yield definite detection of non-zero  $V$  signatures in the LSD lines. Furthermore, the line profile is strongly variable in shape, but not in  $v_r$ . We classify HD 153948 as a definite magnetic Ap star.

The proper motions are consistent with membership in NGC 6281 (Paper II). The position in the HR Diagram is consistent with the cluster isochrone. On the other hand, the radial velocity measured on all three nights, about  $-2.5$  km s $^{-1}$ , is inconsistent with the reported cluster radial velocity of  $-15.4$  km s $^{-1}$  (Kharchenko et al. 2005). However, this value for the cluster radial velocity appears to be based on only one measurement of one star, and is therefore highly uncertain. We disregard this inconsistency, and accept HD 153948 as a probable cluster member.

### 5.7. HD 317857 = NGC 6383-3, A1IVp

Both FORS1 (Paper I) and our single field measurement of this star reveal a strong (kG) field. HD 317857 is certainly a magnetic Ap star. However, both the radial velocity of  $-24$  km s $^{-1}$  measured (once) by Lloyd Evans (1978), and the value of  $-10$  km s $^{-1}$  from our ESPaDOnS spectrum, are inconsistent with the cluster radial velocity of about  $+5$  km s $^{-1}$  reported by Kharchenko et al. (2005); although the two stellar measurements taken together suggest that the star is a spectroscopic binary. More definitively, HD 317857 is about 0.8 dex too bright for the cluster isochrone. It appears that this star is a probable cluster non-member.

### 5.8. HD 318100 = NGC 6405-19, B9p

Both the FORS1 measurement and the present ESPaDOnS observation reveal longitudinal fields of a few hundred G, significant at the several  $\sigma_B$  level. The star also has an extremely large value of the  $\Delta\alpha$  peculiarity parameter (Maitzen & Schneider 1984). HD 318100 is definitely a magnetic Ap.

Kharchenko et al. (2005) report proper motions that are consistent with the cluster mean values; our radial velocity of  $-8$  km s $^{-1}$  is consistent with the cluster mean of  $-7 \pm 1$  km s $^{-1}$  (Kharchenko et al. 2005); and the inferred luminosity (Paper II) is consistent with the cluster isochrone. We consider HD 318100 a member of NGC 6405.

### 5.9. HD 320764 = NGC 6475-23, A1V an

One FORS1 measurement, based mainly on Balmer lines, yielded no field detection with  $\sigma_B = 66$  G. Our two measurements have uncertainties of the order of 4–500 G due to the extremely broad and shallow LSD line, and provide no really useful constraint. Folsom et al. (2007) report  $v_e \sin i = 225$  km s $^{-1}$ , and their abundance analysis shows that this is a normal star, not a magnetic Ap.

Proper motions suggest that this star is a probable cluster member (cf Paper II).

#### 5.10. HD 162576 = NGC 6475-55, B9.5p SiCr

Our three field measurements with ESPaDOnS are the first made of this star. In spite of standard errors as low as about 20 G, none of the measurements of  $\langle B_z \rangle$  are significantly different from zero. However, we have one significant detection of a non-zero  $V$  signature. In addition, the LSD profile is strongly variable, without any change in  $v_r$ . The star has been reported to be photometrically variable (North 1984), and Folsom et al. (2007) report that the abundances found in the atmosphere are clearly typical of magnetic Ap stars. We classify HD 162576 as a magnetic Ap star; it appears to be close to the weak-field limit of such stars (cf Aurière et al. 2007).

Astrometric data indicate that the star is a member of NGC 6475 (cf Paper II), and our measured values of  $v_r$  are consistent with the cluster radial velocity of  $-14.7 \pm 0.2 \text{ km s}^{-1}$  (Robichon et al. 1999). This star is a probable cluster member.

#### 5.11. HD 162588 = NGC 6475-59, Ap Cr

None of our three field measurements (the first such observations of this star) reveal a  $\langle B_z \rangle$  value that is significantly different from zero, but the  $\sigma_B$ s are fairly large, of order 100 G, because of the elevated value of  $v_e \sin i$  ( $70 \text{ km s}^{-1}$ ). No significant  $V$  signal is detected. However, the LSD  $I$  line profile is strongly variable without significant change in  $v_r$ . The star is a photometric variable (North 1984). We have synthesised a small section of the  $I$  spectrum, and find that Cr is overabundant by about 1.5 dex. In spite of the absence of direct evidence for the presence of a magnetic field, we classify the star as a magnetic Ap star.

Astrometric data indicate that HD 162588 is a member of NGC 6475 (Dias et al. 2001). Our measured  $v_r$  values are consistent with the cluster velocity, and we consider the star a cluster member.

#### 5.12. HD 162630 = NGC 6475-63, B9V

No significant  $\langle B_z \rangle$  field was detected in two measurements, and no significant  $V$  signature is present. The LSD profile is considerably deeper using a solar line list than with an Ap line list of the same temperature, which is usually a symptom that many lines present in the Ap list but not in the solar list are actually weak or absent in the analysed star. In addition, the LSD line profile is apparently a simple rotation profile, and it does not vary between our two observations. In the  $I$  spectrum, He I and O I are quite strong, which is normally not the case for magnetic Ap stars. Synthesis of a small section of  $I$  spectrum shows that Fe appears underabundant relative to solar by about 0.3 dex, while Si and He have abundances close to solar. We conclude that HD 162630 is not a magnetic Ap star, but an (approximately?) normal star of  $T_{\text{eff}} \approx 10400 \text{ K}$ .

HD 162630 does appear, both on the basis of proper motions and of our  $v_r$  measurements, to be a member of NGC 6475.

#### 5.13. HD 162656 = NGC 6475-72, B9V

Our single measurement, the first field measurement of HD 162656, shows no sign of a magnetic field either in the value of  $\langle B_z \rangle$  or in the LSD  $V$  profile. The LSD profile is deeper, and the field measurement more accurate, using a solar line list than

with an Ap list. The LSD line profile appears to be broadened simply by rotation. Although the star has a  $T_{\text{eff}}$  value of about 9500 K, the  $I$  spectrum shows strong He I and O I lines, and the Cr II lines near 6150 Å are weak or absent. Synthesis of short sections of the  $I$  spectrum confirms these qualitative observations; He, Si, and Fe all have abundances close to solar, while Cr appears to be about 0.2 dex below solar. We classify this star as normal.

The proper motions are consistent with membership in NGC 6475, but our one measured  $v_r$  value is not. However, it has been reported by Giesekeing (1977) that the star is a spectroscopic binary, and that the  $\gamma$  value of the orbit is consistent with cluster membership. We consider the star to be a cluster member.

#### 5.14. HD 162725 = NGC 6475-88, A0p SiCr

Our data are the first magnetic field measurements of this star. One of our two measurements reveals a  $\langle B_z \rangle$  value  $7\sigma_B$  different from zero, although the other is consistent with zero. Both observations have LSD  $V$  signatures that are clearly different from zero. Folsom et al. (2007) report that the atmospheric composition of HD 162725 is clearly that of an Ap star. The star is also a photometric variable (North 1984). It is clear that this star is a magnetic Ap star.

Both proper motions and our radial velocity are consistent with classification of the star as a member of NGC 6475.

#### 5.15. HD 169842 = NGC 6633-39, A1p SrCr

Kudryavtsev et al. (2006) report probable detection of a field of  $B_{\text{rms}} \approx 370 \text{ G}$  from five measurements with typical standard errors of about 180 G. Our three observations provide clear detections of  $\langle B_z \rangle$  at about the  $10\sigma_B$  level, and confirm the general magnitude of the field reported by Kudryavtsev et al. Synthesis of two spectral windows (cf. Figure 1) indicates that Cr is overabundant relative to solar abundances by about 2 dex, while Si and Fe are near solar abundances. HD 169842 is definitely a magnetic Ap star.

Proper motions are consistent with membership in NGC 6633. The cluster radial velocity is reported by Kharchenko et al. (2005) to be between  $-25$  and  $-29 \text{ km s}^{-1}$ . Individual radial velocities from references cited in WEBDA support a value around  $-29 \text{ km s}^{-1}$ . Our measured  $v_r$  values are consistent with these values, and we consider the star to be a cluster member.

#### 5.16. HD 169959A = NGC 6633-58, A0p Si

The field of this star was first detected with FORS1 (Paper I). Our field measurement confirms the presence of a field and its general magnitude in this magnetic Ap star.

The proper motions and previous radial velocity measurements (Hintzen et al. 1974) are consistent with membership in NGC 6633. However, our one radial velocity ( $-53 \text{ km s}^{-1}$ ) is inconsistent with both the cluster velocity of about  $-30 \text{ km/s}$  and with the measurements of Hintzen et al. It is not at all clear what the origin of this discrepancy is. Furthermore, HD 169959A, if it is a cluster member, is a (very) blue straggler. We conclude that it is a probable cluster non-member.



### 5.17. HD 170054 = NGC 6633-77, B6IV

No field was detected in two previous FORS1 measurements with standard errors of about 75 G (Paper I). Our two new measurements, one with a larger  $\sigma_B$  (due to a period of low transparency) and one with smaller  $\sigma_B$  also reveal no field, nor is there any hint of a field in the  $V$  signatures. Spectral lines of He I, O I, and Ne I are strong, while Cr and Fe appear roughly normal. Synthesis confirms abundances of He and Fe that are close to solar, while Si appears about 0.2 dex below solar. We classify HD 170054 as a normal B star, although the peculiar shapes of the  $I$  line profiles, and their variability, suggest that this star may be a pulsating variable.

Proper motions indicate that the star is a cluster member, and our  $v_r$  value is consistent with this. We consider the star to be a cluster member.

### 5.18. HD 170860 = IC 4725-153, B9IV/Vp

The magnetic field of this star was not detected in one FORS1 measurement, which achieved  $\sigma_B = 69$  G. Our single ESPaDOnS measurement nominally provides about a  $2\sigma_B$  detection, although both  $\langle B_z \rangle$  and  $\sigma_B$  are not very well determined, due to uncertainties as to where the edges of the LSD line profile are. However, a large and clearly significant  $V$  signature is present. In addition, the  $\Delta a$  value (Maitzen 1985) is rather large, providing further support to our classification of this star as a magnetic Ap star.

Proper motions indicate that HD 170860 is a member of IC 4725. The mean cluster radial velocity has been reported as having values from  $-4 \pm 4$  (Feast 1957) to  $+2.4 \text{ km s}^{-1}$  (Kharchenko et al. 2005). Because of the difficulty of determining the centroid of the LSD line, our  $v_r$  value is not derived from this line; instead, it is derived by fitting Gaussians to the cores of the Balmer lines  $H\alpha - H\delta$ , and the strong Si II lines 4128-30 and 6347-71 Å. The value found by us,  $-13 \pm 3 \text{ km s}^{-1}$ , is not the same as the cluster mean, but with only one measurement, we cannot rule out the possibility that the star is a spectroscopic binary. We regard HD 170860 as a probable cluster member.

### 5.19. HD 172271 = IC 4756-118, A0p Cr

Our measurement is the first reported magnetic observation of this star. We find a marginally significant  $\langle B_z \rangle$  in this star. The significantly peculiar value of the Geneva index  $Z = -0.027$ , and the apparent absence of He I lines in HD 172271, strongly suggest classification as a magnetic Ap star. This is confirmed by synthesis of a small spectral region, from which we find that Cr is overabundant by about 2.5 dex, while Fe is about 0.5 dex overabundant.

The value of  $\mu_\alpha \cos \delta$  is about  $2\sigma$  from the cluster mean, but  $\mu_\delta$  is consistent with membership. The cluster  $v_r$  is  $-25.8 \pm 0.2 \text{ km s}^{-1}$  (Robichon et al. 1999; note sign error on their  $v_r$  value); our measured  $v_r = -21 \pm 2 - 3 \text{ km s}^{-1}$  (the star has a large  $v_e \sin i$ ) is reasonably consistent with this value. We regard this star as a probable cluster member.

### 5.20. HD 205073 = NGC 7092-69, A1

Our two measurements of this star are the first reported magnetic observations. No field is detected, either in the  $\langle B_z \rangle$  values or in the  $V$  profiles. Considering the rather small  $v_e \sin i$  value ( $16 \text{ km s}^{-1}$ ), the lack of detection is strong evidence that this

star is not a magnetic Ap. Furthermore, the field measurement is more precise using a solar composition line list for LSD analysis. Neither the  $\Delta a$  nor the Geneva  $Z$  peculiarity indices are significantly different from zero, and our spectra show line profiles which appear to be simply rotationally broadened, with clearly present He I and O I but very weak Cr II and no rare earths. The abundances of Cr and Fe deduced from spectrum synthesis of small sections of the spectrum are close to solar. It is clear that this star is a normal A star. Note incidentally the two quite different  $v_r$  values of the two observations; HD 205073 is a spectroscopic binary. Since close binaries are rare among magnetic Ap stars, the radial velocity variability supports our view that HD 205073 is not such a star.

The proper motions are consistent with cluster membership (Baumgardt et al. 2000; Dias et al. 2001). We consider the star to be a cluster member.

### 5.21. HD 205331 = NGC 7092-118, A1V

The first published magnetic measurements of this star were those of Kudryavtsev et al. (2006), who failed to detect a field in three observations with  $\sigma_B$  of about 280 G. Our three data reduce the standard error to the 30 – 40 G range. We do not have a statistically significant detection in the  $V$  signature in any of the three observations, but one  $\langle B_z \rangle$  value (integrated over the whole broad line) is about  $3\sigma_B$  different from zero, and suggests a field of about 140 G. However, our field measurement is as precise with a solar line list as with an Ap list, and the LSD profile appears to be due to pure rotational broadening. Both these features are often signatures of a normal star. Our spectra show a clear He I  $\lambda 5875$  line (in spite of the low  $T_{\text{eff}}$  value), strong O I, weak Cr II, and no obvious rare earths. The brightness is constant in the Hipparcos photometry catalogue. Synthesis of two short spectral regions in the ESPaDOnS  $I$  spectrum yields near-solar abundances of Si, Cr and Fe, assuming that the microturbulence parameter is about  $2 \text{ km s}^{-1}$ . We classify HD 205331 as a normal star of  $T_{\text{eff}} \approx 9450 \text{ K}$  in spite of the single apparently significant field detection.

The proper motions and parallax are consistent with cluster membership (Baumgardt et al. 2000; Dias et al. 2001). The accurate cluster radial velocity of  $-5.4 \pm 0.4 \text{ km s}^{-1}$  (Robichon et al. 1999) is agrees with the three values of  $v_r$  measured by us. We consider the star a cluster member.

### 5.22. BD +49 3789 = NGC 7243-490, B7p Si

Our single measurement of the field of this star is the only one available. The precision is very low ( $\sigma_B \sim 400 \text{ G}$ ), and no detection is achieved. The large values of the photometric peculiarity indicators  $\Delta a$  and Geneva  $Z$ , and the presence of strong Si II lines in our  $I$  spectrum suggest that BD +49 3796 is actually a magnetic Ap star. This view is confirmed by synthesis of two small spectral windows, which yields an underabundance of He by about 1 dex, and overabundances of Si, Cr and Fe by respectively 1, 0.7, and 0.5 dex relative to solar abundances.

Astrometric data for this star, and HR Diagram position, are consistent with cluster membership, but our single  $v_r$  value differs from the cluster mean of between  $-9 \text{ km s}^{-1}$  (Hill & Barnes 1971) and  $-13 \text{ km s}^{-1}$  (Kharchenko et al. 2005) by about  $5 \text{ km s}^{-1}$ . However, Hill & Barnes report four  $v_r$  measurements between  $-13$  and  $+32 \text{ km s}^{-1}$ , and consider the star a spectroscopic binary. We regard the star as a probable member.

### 5.23. HIP 109911 = NGC 7243-370, A0Vp Si

Our magnetic measurement is the only one available for this star, and does not reveal a significant  $\langle B_z \rangle$  or  $V$  signal, although there is a hint in our low-precision  $2\sigma_B \langle B_z \rangle$  that there might be a field of a few hundred G present. In any case, the photometric peculiarity indices  $\Delta a$  and Geneva  $Z$  are large enough to strongly suggest that HIP 109911 is a magnetic Ap, and the obvious strength of Si II and Cr II lines supports this view. Synthesis of a small spectral window yields He depleted by 1.5 dex, and Si and Fe enhanced by 1 and 1.2 dex respectively relative to solar. We classify the star as a magnetic Ap star.

The proper motions (Baumgardt et al. 2000; Dias et al. 2001) and position in the HR Diagram are consistent with cluster membership. Hill & Barnes (1971) report four  $v_r$  values between  $-8$  and  $-24 \text{ km s}^{-1}$  but do not flag the star as a velocity variable, perhaps reflecting the relatively large mean errors. Our single  $v_r$  value, with an uncertainty of roughly  $2 \text{ km s}^{-1}$ , is consistent with membership. We consider the star a cluster member.

## 6. Characteristics of the data set

In three nights (of which all but a few hours were clear) with ESPaDOnS we have obtained 44 observations of 23 stars which are possible magnetic Ap stars *and* possible members of open clusters. For 12 of these 23 stars, our measurements represent the first published magnetic data.

Because of the time of year when our observing run was scheduled, about half of our ESPaDOnS observations were made on stars which had been previously observed, either earlier in our cluster survey with FORS1 (Paper I), or by others. Nevertheless, the data we have acquired provide valuable new information about possible cluster magnetic stars, even when these stars have been previously measured for magnetic fields.

One important class of information provided by our new ESPaDOnS data is accurate radial velocities of almost all the stars observed. Because the usefulness of proper motions as a discriminant of cluster membership diminishes roughly proportionally to distance (the required accuracy of motions increases with distance, but the uncertainties of available data set remain roughly constant), while radial velocities continue to be a precise discriminant to whatever distance they can be measured accurately, the radial velocities are particularly useful in testing membership of stars in clusters that are more than  $1 - 200 \text{ pc}$  distant. For all but a few of the 23 stars observed, our data provide a valuable test of membership, mostly supporting cluster membership. However, our  $v_r$  data indicate that two stars previously thought to be cluster members (HD 317857 and HD 169959A) are probable non-members.

Another important type of information provided by ESPaDOnS is clearer discrimination between stars which are magnetic Ap stars with fields small enough to be difficult to detect, and stars which are not magnetic Ap stars. In order to obtain representative field strength *distributions* for various star masses and ages, we have included a number of stars in which fields have not yet been detected, but for which other evidence exists indicating that they are probably magnetic Ap stars, in the sample analysed in Paper II. Even with ESPaDOnS observations of such stars it is not always possible to detect or rule out a field, but in most cases the ESPaDOnS spectrum allows one to classify a star with confidence as either a magnetic Ap or a normal star, something which is not usually possible with FORS1  $I$  spectra (see for example the discussions of HD 162630, HD 162656, HD 170054, HD 205073, and HD 205331). Our  $I$  and  $V$  spec-

tra allow us to categorise nine stars of the present sample as not magnetic Ap stars; in most cases, these appear to be normal stars.

One obvious aspect of the present data set is that in stars with relatively rich and sharp-lined metal spectra, ESPaDOnS data may allow the detection of fields not readily detected with FORS1. Of the two stars for which we report the first direct evidence of a magnetic field, one (HD 162725) was previously observed with FORS1 (Paper I).

Of course, for all the stars we observe, the new measurements contribute to convergence of  $B_{\text{rms}}$ , the RMS longitudinal field (see Paper II and below), which is the measure we use of the global characteristic field strength of each star in our sample.

## 7. Magnetic field evolution through the main sequence

We next use the new data acquired from ESPaDOnS to revise our global database of magnetic Ap stars that are members of clusters. We flag stars that are found to be probable or certain non-members, or probable or certain non-magnetic stars. We add newly studied probable or certain magnetic cluster Ap stars to the database. For each of the new stars, we determine the fundamental parameters  $T_{\text{eff}}$  and  $\log(L/L_{\odot})$  using the same techniques as in Paper II. As discussed in detail in that paper, we assume that the uncertainty in  $\log(T_{\text{eff}})$  is  $\pm 0.02$ , and the uncertainty in  $\log(L/L_{\odot})$  is  $\pm 0.1$ . With these data, we place each star in the cluster HR diagram, check whether its position in the HR diagram is close enough to the cluster isochrone to be consistent with membership, and estimate its mass from its position.

For each retained magnetic cluster member (old or new) in the database for which we have new magnetic data, we compute the revised characteristic field strength  $B_{\text{rms}}$ , which is simply the RMS average of all available field measurements, or the subset with the smallest uncertainties. (Although  $B_{\text{rms}}$  is a fairly crude measure of stellar field strength, it is the best measure we can easily form from the data until enough is known about most stars in the sample to actually compute simple models of individual field structure.) Finally, we re-examine the evolution of magnetic fields with time elapsed on the main sequence to see if any of the conclusions of Paper II have to be modified.

After carrying out these steps, we find that we have 12 stars which satisfy our criteria of cluster membership and probable or definite magnetic Ap nature, and for which the magnetic field data are new or improved, so that a new value of  $B_{\text{rms}}$  may be calculated. These stars are listed in Table 5. The table is similar to Table 3 of Paper II in the information it contains. For each magnetic Ap cluster member for which new magnetic data have been obtained, the table lists the cluster to which the star belongs, the cluster age and uncertainty (see below), the true (not apparent) distance modulus  $DM$  of the cluster, the star identification, the star's  $\log(T_{\text{eff}})$ ,  $\log(L/L_{\odot})$ ,  $M/M_{\odot}$  with uncertainty, fractional age  $\tau$  with uncertainty, the revised value of  $B_{\text{rms}}$ , and the number  $n_B$  of magnetic observations contributing to  $B_{\text{rms}}$ . (Note that for Ap stars for which we have not yet detected a field, we use only the most accurate measurements in forming  $B_{\text{rms}}$ , so as not to inflate that parameter by including numbers with unnecessarily large uncertainties.)

We also use the newly measured stars to test the cluster ages found in the literature by comparing the position of stars near the terminal age main sequence (TAMS) with the isochrones. In Paper II, we found that this procedure made it possible to improve the precision of age determination of several open clusters. Compared to Paper II, we obtain improved ages with smaller er-

ror bars for NGC 6475, IC 4725, and IC 4756. These improved ages are listed in column 2 of Table 5.

Then finally we include the new data together with the data from Paper II to check whether the new magnetic measurements alter our previous conclusions (Paper II) concerning the evolution of magnetic fields with time through the main sequence lifetime of magnetic Ap stars. The full, revised data set of stars which are probable cluster members, probable Ap stars, and for which at least one field measurement is available, is used to create Figure 4, which contains information similar to that found in Figure 5 of Paper II.

In this figure the RMS field estimates  $B_{\text{rms}}$  for individual stars (in three mass bins:  $2 - 3 M/M_{\odot}$ ,  $3 - 4 M/M_{\odot}$ , and  $4 - 5 M/M_{\odot}$ , bins for which a significant number of stars are now available) are plotted as a function of cluster (and thus of stellar) age (left three panels) and of fractional age (right three panels). The full sample is divided into mass bins in order to be able to study the variation of typical field strength  $B_{\text{rms}}$  with stellar age as a function of stellar mass. (Note that the star NGC 2244-334, with  $B_{\text{rms}} = 9515$  G,  $\log(\text{age}) = 6.40$ , and  $\tau = 0.02$  is off-scale in the upper left corner of both bottom panels.)

The present sample differs from the sample of Paper II essentially in that the first magnetic measurements for five stars have been added, and the  $B_{\text{rms}}$  data for five other stars have changed, always by a factor of less than two. Although the ESPaDOnS data do not increase the total size of the sample very much, these observations have substantially increased the information available about lower-mass Ap stars that have completed a large part of their main sequence evolution (see the fractional age column of Table 5). These data provide a significant improvement for a region of parameter space that was not very well represented in the previous sample.

The data of the full sample of probable cluster magnetic Ap stars are displayed here a little differently than in Paper II. In Figure 4 we show the variation of  $B_{\text{rms}}$  (rather than its logarithm) as a function of stellar (= cluster) age in the left panels, and as a function of fractional age in the right panels. The three panels in each column show the data for the three mass bins mentioned above. In all three right-hand panels we can now see clearly that RMS fields larger than 1 kG are common at small fractional age, while the (now numerous) stars of fractional ages larger than about 0.4 for  $2 - 3 M_{\odot}$ , 0.2 for  $3 - 4 M_{\odot}$ , and 0.1 for  $4 - 5 M_{\odot}$  have fields that are always less than 1 kG. These trends are not so easily seen in the left panels using  $\log(\text{age})$  as the abscissa, which expand the region of small fractional age at the expense of regions of large fractional age, but close examination of the left panels shows that the same effect is present. In all three panels on the left side of the figure, a significant number of low field stars (but no high-field stars) are present near the TAMS.

The obvious interpretation of this figure is that the RMS field declines rather sharply with age after a characteristic time which is of the order of 250 Myr for stars in the mass range  $2 - 3 M_{\odot}$ , 40 Myr for  $3 - 4 M_{\odot}$ , and 15 Myr for  $4 - 5 M_{\odot}$  stars. It is remarkable that the characteristic time of the field decreases rapidly as the stellar mass increases, *both* in absolute value and as a fraction of the stellar main sequence lifetime.

One expected physical effect which would lead to some substantial decline in surface magnetic field is of course the geometric expansion of the stars by a factor of about two in radius as they evolve from the ZAMS to the TAMS. If magnetic flux (and global field topology) are approximately conserved, the increase of radius by a factor of order two will lead to decrease in field strength by a factor of order four. We test this possibility by plotting  $B_{\text{rms}} \times (R/R_{\odot})^2$  for the stars of Figure 4 as a function of

$\log(\text{age})$  and  $\tau$  in Figure 5. This quantity is a reasonable proxy for the emergent or apparent magnetic flux (normalised to an average field of 1 G over a star of one  $R_{\odot}$ ); it differs from the true normalised emergent flux by a factor (dependent on the viewing geometry and obliquity of the stellar field) which relates the RMS value of the observed sample of values of mean longitudinal field  $\langle B_z \rangle$  to the typical field modulus at the stellar surface. This factor is at least about 3, and is likely to be of the order of 5 for most of the stars of our sample. Of course, the emergent flux may or may not be closely related to the flux deep in the stellar interior. However, note that fields *are* detected among the older stars in all our mass bins. The fields decline in all bins, but not to zero in the main sequence lifetime of the stars considered.

Overall we see that Figure 5 shows much the same behaviour as Figure 4. Near  $\tau = 0$  there is a rather large range of estimated normalised emergent magnetic fluxes, and a few stars which exceed the median normalised flux value by a factor of 10 or more. As one moves towards larger fractional age, the fluxes converge on lower values – quickly for the higher mass ranges, more slowly for the (top)  $2 - 3 M_{\odot}$  bin. From the right column of figures, one plausible hypothesis is that stars with initially low fields, less than about 1 kG, tend to conserve flux as they evolve across the main sequence. However, the stars with initially large fields, those that contribute the large normalised flux values in the figure, appear to lose much of this flux within a time short compared to the main sequence lifetime. This flux loss is *not* due to the geometric expansion of the star, already taken into account in the method of estimating the normalised magnetic flux. Instead, it could be some kind of relaxation or redistribution process.

We do not find any analogues of the young, high-field (and high emergent flux) stars among the (now reasonably numerous) older stars in any of the mass bins considered here. We conclude that the present data may be consistent with approximate emergent flux conservation in most magnetic Ap stars, but that the initially high-field stars seem to suffer a real decline in the total emergent magnetic flux during the main sequence phase of evolution. Alternatively, the present data may show that typical emergent magnetic flux declines significantly in most or all stars (rather than only in the stars with initially large fields and fluxes), by a factor of two or three, during the main sequence phase.

It appears that our observations are consistent with the fossil field hypothesis (as we have implicitly assumed in discussing the possibility of flux conservation above), in that the flux in older stars are within a factor of two or three of the fluxes in young stars in each mass bin. As many authors have noted, these fluxes do not show the expected correlation with rotation that is found in the presumably dynamo-generated fields of lower main sequence stars. In fact, some of the largest fields are found among stars that rotate very slowly.

Furthermore, one theoretical concern about the fossil field hypothesis has been the question of whether fossil fields are stable over long time scales. Tayler (1973), Markey & Tayler (1973; 1974), and Wright (1973) have shown that fields which are purely poloidal or purely toroidal in the radiative interior of a star are unstable on time-scales that are short compared to the main sequence lifetime of an Ap star. The fact that we find fields with similar fluxes at all ages in each mass bin certainly suggests that, if these fields are fossils, nature has been able to resolve this problem.

This problem has recently been clarified on the basis of a set of important calculations discussed by Braithwaite & Spruit (2004) and Braithwaite & Nordlund (2006). This study has been primarily focussed on the issue of the long-term stability of fos-

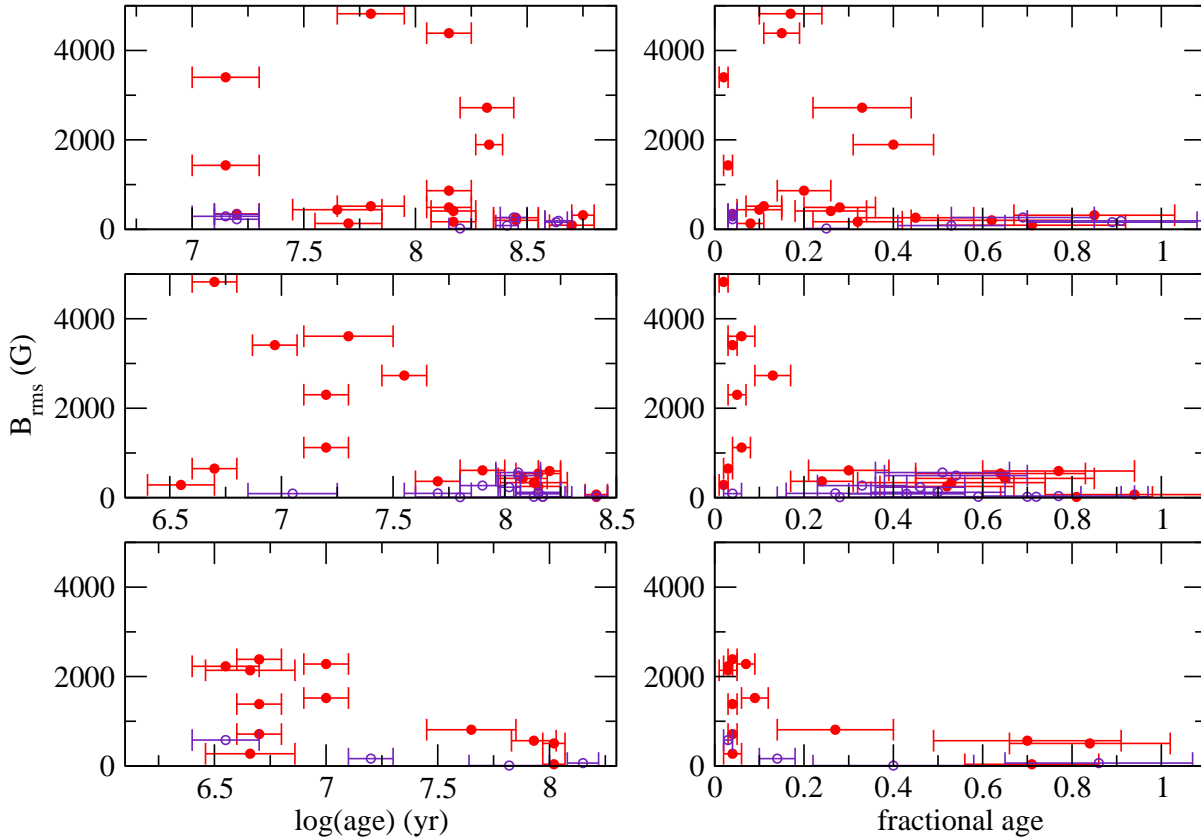


**Fig. 4.** This figure shows the currently estimated values of  $B_{\text{rms}}$  as functions of logarithmic stellar age (left) and of fractional age (right) for three mass bins, from top to bottom  $2-3M_{\odot}$ ,  $3-4M_{\odot}$ , and  $4-5M_{\odot}$ . Filled symbols are stars for which a field is definitely detected; open symbols are probable magnetic Ap stars in which no field has yet been detected. The right-hand limit of each of the panels using  $\log(\text{age})$  as abscissa is near the main sequence lifetime for stars in that mass range. In the bottom pair of panels, one point (for NGC 2244-334) has such a large field ( $B_{\text{rms}} = 9.52 \text{ kG}$ ) that it is off scale (at  $\log t = 6.4 \pm 0.10$  and  $\tau = 0.02 \pm 0.01$  respectively).

sil magnetic fields in Ap stars (and magnetic white dwarfs). These authors conclude, on the basis of numerical simulations of field evolution in a non-rotating polytropic star, that the instabilities found in earlier work lead to rapid field evolution which generally creates a mixed poloidal-toroidal field structure with a twisted toroidal field. Once formed, this structure appears to be stable on a longer time-scale. This work appears to provide confirmation that stable fossil field structures exist, and can be achieved by a star starting from a variety of initial fields, in agreement with the observations of fields with comparable fluxes (to within plus or minus an order of magnitude) in Ap stars of all main sequence ages.

Since this work studies the evolution of field structure in radiative stars similar to main sequence stars, it also leads to predictions of how a global fossil magnetic field should evolve with time, at least under the hypotheses adopted in the model. The evolution found by Braithwaite and collaborators, when their computations are rescaled to approximately realistic magnetic diffusivities, is that the emergent flux gradually grows with time, by a factor that may be of order ten, until finally the main toroidal flux tube begins to emerge from the star, at which point the surface field declines rapidly. (The emergent flux is mostly poloidal, since a stellar atmosphere does not support the large current densities needed for a strong surficial toroidal field component.) This evolution is estimated (roughly) to take somewhat longer than the main sequence lifetime of most Ap stars. Thus these

computations predict that we should mainly see stars in the phase of surface field strength *increasing* with time.

This is, of course, the opposite of the situation revealed by our data, in which we see both field and flux decline with time, at least in some stars and perhaps in all. Thus it appears that the field evolution predicted by the numerical modelling of Braithwaite and collaborators is not fully consistent with observations. The observations *are* consistent in that fields appear to be stable on a long enough time scale to persist throughout the main sequence phase, in agreement with the numerical models, but the observed and computed fields appear to have somewhat different time evolution.

However, it is perhaps not very surprising that the field evolution predicted by these numerical models differs from what is observed. This modelling neglects two effects that may significantly affect the evolution of surface fields. First, the computations are for *non-rotating* stars. The effect of reasonably rapid rotation (and most magnetic Ap stars, including most of the stars in our study, have rotational periods of a few days, and equatorial velocities of several tens of  $\text{km s}^{-1}$ ) is to produce meridional circulation. In turn, this circulation transports angular momentum and almost certainly produces shear within the star. This shear will certainly strongly distort the internal field, which will probably substantially alter the emergent flux. Secondly, the modelling has been carried out for a star of constant size and structure. During the main sequence phase, a real star changes its overall structure significantly, and in particular increases in ra-

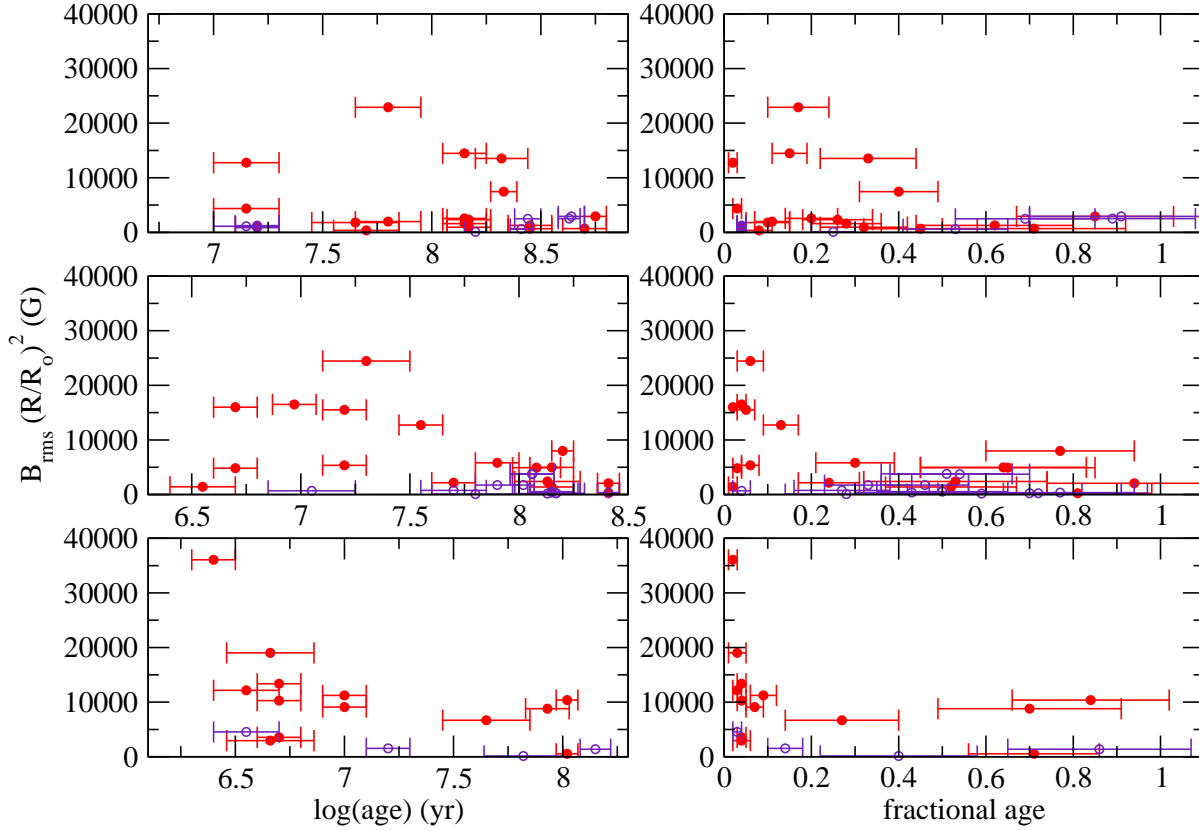


**Fig. 5.** This figure shows the estimated values of normalised emergent magnetic flux  $\sim B_{\text{rms}} \times (R/R_{\odot})^2$  as functions of logarithmic stellar age (left) and of fractional age (right) for three mass bins. Apart from the quantity plotted, this figure has the same structure as Figure 4.

dus by a factor of order two. This radius increase will counteract to some extent the increases surface field strength (although not the increased surface flux). It appears that further computations of field evolution, with incorporation of additional physics, will be of great interest.

## 8. Conclusions

In order to study the evolution of magnetic field strength and of atmospheric chemistry in magnetic Ap stars through their main sequence lifetimes, we have been carrying out a large survey of such stars in open clusters. As discussed in Papers I and II, the main interest of such a sample is the fact that the ages of such stars, especially during the first half of their main sequence lifetime, can be determined with considerably greater precision than is the case for magnetic Ap stars in the nearby field.

Most of the survey so far has been carried out using FORS1 at the ESO VLT (cf Paper I), with an important contribution from earlier studies of the Ori OB1 and Sco OB2 associations (see for example Borra 1981 and Thompson et al. 1987). In this paper we discuss the first use of the new instrument ESPaDOnS at the Canada-France-Hawaii Telescope for this survey. The three nights of data so far obtained from this instrument have made an important additional contribution to the overall survey. They have also made possible several very important checks of previous data, and provided kinds of information not readily available from the lower resolution FORS1 spectra.

Comparison of ESPaDOnS and FORS1 measurements of the same stars show that for stars that are not too hot (say below about 12–13 000 K) and that have  $v_e \sin i$  less than roughly

60 km s<sup>-1</sup>, the precision in  $\langle B_z \rangle$  obtainable with ESPaDOnS in a given time on target is comparable to, and sometimes substantially better than, the precision obtained with FORS1, even though the CFHT has only about 20% of the collection area of one VLT unit telescope. This is possible essentially because ESPaDOnS has far higher resolving power (65 000 compared to 2 000 or less) than FORS1, and thus can fully exploit the Zeeman signal contained in the metal lines. If the star is rotating slowly enough, and is cool enough, this gives ESPaDOnS a very large advantage over FORS1 observations, which must rely to a large extent on the signal in the Balmer lines.

In addition, with ESPaDOnS we have the possibility of detecting a real and significant circular polarisation  $V$  signal in the averaged line profile even if the mean longitudinal field  $\langle B_z \rangle$  is close to zero. In weak-field stars such as HD 108945 the field is much easier to detect this way than through conventional measurements of  $\langle B_z \rangle$ . This capability is also very helpful in deciding which proposed Ap stars in a cluster are in fact Ap stars, and which are normal or belong to other, non-magnetic, peculiarity classes. Having clear evidence on this point is very helpful in cleaning the field measurement sample of non-magnetic stars.

Furthermore, with ESPaDOnS we obtain not only spectropolarimetry, but also high-resolution  $I$  spectra over a wide wavelength window. These data are very useful for deciding which stars have the chemical peculiarities of magnetic Ap stars, and which appear chemically more or less normal. We have exploited this possibility above to eliminate some stars that have been suggested as magnetic Ap stars from the survey sample. In a later stage of this project, we plan to model in detail a number of the  $I$  spectra from ESPaDOnS with the goal of obtaining a clearer

picture of the evolution of atmospheric chemical peculiarities during the main sequence lifetime of such stars. This cannot be done at present with useful accuracy for the low resolution spectra obtained with FORS1.

The accurate radial velocities that can be obtained with ESPaDOnS (recall that the precision of radial velocities, for stars with  $v_e \sin i$  of the order of  $50 \text{ km s}^{-1}$ , sometimes with non-symmetrical LSD profiles, is roughly  $\pm 1 - 2 \text{ km s}^{-1}$ ) provide valuable tests of cluster membership for stars of our sample. The accuracy of radial velocity measurements from our FORS1 data is probably not good enough to provide really useful constraints.

The precision of the best field measurements obtained with ESPaDOnS is extremely high. The best measurement have standard errors in the range of 15–30 G, as small as or smaller than the highest precision (about 30 G) that has been obtained reliably with FORS1. This has made it possible to add five new stars to the sample of cluster Ap stars with field measurements, and to add further measurements of several others stars of the sample. The new measurements provide valuable additional data on stars having low mass and large fractional ages  $\tau$ , a part of the sample which was under-represented in our previous data set.

We have re-examined the full sample, and present the data in a somewhat different form than in Paper II. We find that our earlier conclusions (see Paper II) are somewhat altered. As before, we find that magnetic fields of stars with masses above about  $3 M_\odot$  decline rather strongly through the main sequence life, dropping in strength by a factor of several after about  $4 \cdot 10^7 \text{ yr}$  and  $1.5 \cdot 10^7 \text{ yr}$  for stars in the  $3 - 4$  and  $4 - 5 M_\odot$  bins respectively. This is consistent with the  $3 \cdot 10^7 \text{ yr}$  found for stars above  $3 M_\odot$  in Paper II. However, in contrast to the results of Paper II, we now find clear evidence that the fields of lower mass Ap stars ( $2 - 3 M_\odot$ ) appear to decline with increasing age after roughly  $2.5 \cdot 10^8 \text{ yr}$ . Furthermore, for all masses, the data suggest that even the emergent magnetic *flux* either declines somewhat in all stars through the main sequence lifetime, or that the emergent flux in the more strongly magnetic stars found at young fractional ages is somehow reduced.

When our results are compared with the numerical computations of Braithwaite & Spruit (2004) and Braithwaite & Nordlund (2006), the data are found to support the numerical results in that both observations and numerical simulations agree that the apparently fossil fields of magnetic Ap stars are stable on an evolutionary time scale. On the other hand, the numerical models predict that during the main sequence phase the typical magnetic fields of Ap stars should be observed to *increase*, the opposite of what is observed. However, since these computations neglect both the internal (poloidal and toroidal) circulation flows induced by rotation (which will probably strongly distort the field), and the global radius increase as the star evolves from ZAMS to TAMS, it is quite possible that the evolutionary predictions will be substantially modified as more physics is included in the modelling. It will be of great interest to see whether including these (or other) physical effects in the numerical models leads to more complete agreement between computation and observation.

We are continuing our survey, both to obtain more precise values of the characteristic field strength indicator  $B_{\text{rms}}$  used in this study for stars already observed, and to increase the sample to a larger number of clusters and stars. Our ultimate goal is to provide clear and unambiguous observational constraints on the evolution of both magnetic field strength (and perhaps even structure), and of atmospheric chemistry, through the main sequence lifetime of the magnetic Ap and Bp stars.

**Acknowledgements.** We thank the anonymous referee for helpful comments and suggestions. Work by JDL, JS, JS, and GAW has been supported by the Natural Sciences and Engineering Research Council of Canada. GAW has also been supported by the ARP programme of DND Canada. LF has received support from the Austrian Science Foundation (FWF project P17980-N2). SVB acknowledges the EURIY Award from the ESF/SNF and research grant 115417 from the Academy of Finland. This work is based on data collected at the Canada-France-Hawaii Telescope. Our research has made use of the SIMBAD database, operated at CDS, Strasbourg, France, of the WEBDA open cluster database, created at the EPFL and now hosted at the Institute of Astronomy of the University of Vienna, and of the Vienna Atomic Line Database VALD.

## References

- Aurière, M., Wade, G. A., Silvester, J., Lignières, F., Bagnulo, S., et al. 2007, submitted to A&A
- Babcock, H. W. 1947, ApJ 105, 105
- Bagnulo, S., Hensberge, H., Landstreet, J. D., Szeifert, T., Wade, G. A. 2004, A&A 416, 1149
- Bagnulo, S., Landstreet, J. D., Mason, E., Andretta, V., Silaj, J., Wade, G. A. 2006, A&A 450, 777 (Paper I)
- Baumgardt, H., Dettbarn, C., Wielen, R. 2000, A&AS 146, 251
- Borra, E. F. 1981, ApJ 249, L39
- Borra, E. F., Landstreet, J. D., Thompson, I. 1983, ApJS 53, 151
- Braithwaite, J., Spruit, H. C. 2004, Nature 431, 819
- Braithwaite, J., Nordlund, Å. 2006, A&A 450, 1077
- Bychkov, V. D., Bychkova, L. V., Madej, J. 2003 A&A 407, 631
- de Zeeuw, P. T., Hoogerwerf, R., de Bruine, J. H. J., Brown, A. G. A., Blaauw, A. 1999, AJ 117, 354
- Dias, W. S., Lépine, J. R. D., Alessi, B. S. 2001, A&A 388, 168
- Donati, J.-F., Semel, M., Carter, B. D., Rees, D. E., Cameron, A. C. 1997, MNRAS 291, 658
- ESA 1997, The Hipparchos and Tycho Catalogues, ESA SP-1200
- Feast, M. W. 1957, MNRAS 117, 193
- Folsom, C. P., Wade, G. A., Bagnulo, S., Landstreet, J. D. 2007, MNRAS 376, 361
- Gieseking, F. 1977, A&A 60, 9
- Hill, G., Barnes, J. V. 1971, AJ 76, 110.
- Hintzen, P., Scott, J., Whelan, J. 1974, ApJ 194, 657
- Høg, E., Fabricius, C., Makarov, V. V., Urban, S., Corbin, T., Wycoff, G., Bastian, U., Schwendendiek, P., Wicenc, A. 2000a, A&A, 355, L27
- Høg, E., Fabricius, C., Makarov, V. V., Bastian, U., Schwendendiek, P., Wicenc, A., Urban, S., Corbin, T., Wycoff, G. 2000b, A&A, 357, 367
- Jones, B. F., Fischer, D., Shetrone, M., Soderblom, D. R. 1997, AJ 114, 352
- Kharchenko, N. V., Piskunov, A. E., Röser, S., Schilbach, E., Scholz, R.-D. 2005, A&A 438, 1163
- Kudryavtsev, D. O., Romanyuk, I. I., Elkin, V. G., Paunzen, E. 2006, MNRAS 372, 1804
- Kochukhov, I., Bagnulo, S. 2006, A&A 450, 763
- Kupka, F., Piskunov, N. E., Ryabchikova, T. A., Stempels, H. C., Weiss, W. W. 1999, A&AS 138, 119
- Landstreet, J. D. 1982, ApJ 258, 639
- Landstreet, J. D. 1988, ApJ 326, 967
- Landstreet, J. D., Bagnulo, S., Andretta, V., Fossati, L., Mason, E., Silaj, J., Wade, G. A. 2007, A&A 470, 685 (Paper II)
- Lloyd Evans, T. 1978, MNRAS 184, 661
- Maitzen, H. M. 1985, A&AS 62, 129
- Maitzen, H. M. 1993, A&AS 102, 1
- Maitzen, H. M., Schneider, H. 1984, A&A 138, 189
- Markey, P., Tayler, R. J. 1973, MNRAS 163, 77
- Markey, P., Tayler, R. J. 1974, MNRAS 168, 505
- Norris, J. 1971, ApJS 23, 213
- North, P. 1984, A&AS 55, 259
- Piskunov, N. E., Kupka, F., Ryabchikova, T. A., Weiss, W. W., & Jeffery, C. S. 1995, A&AS 112, 525
- Robichon, N., Arenou, F., Mermilliod, J.-C., Turon, C. 1999, A&A 345, 471
- Ryabchikova, T. A., Piskunov, N. E., Stempels, H. C., Kupka, F., & Weiss, W. W. 1999, Phys. Scr. T83, 162
- Shorlin, S. L. S., Wade, G. A., Donati, J.-F., Landstreet, J. D., Petit, P., Sigut, T. A. A., Strasser, S. 2002, A&A 392, 637
- Tayler, R. 1973, MNRAS 161, 365
- Thompson, I. B., Brown, D. N., Landstreet, J. D. 1987, ApJS 64, 219
- Wade, G. A., Donati, J.-F., Landstreet, J. D., Shorlin, S. L. S. 2000a, MNRAS 313, 823
- Wade, G. A., Donati, J.-F., Landstreet, J. D., Shorlin, S. L. S. 2000a, MNRAS 313, 851



- Wade, G. A., Aurière, M., Bagnulo, S., Donati, J.-F., Johnson, N., Landstreet, J. D., Lignières, F., Marsden, S., Monin, D., Mouillet, D., Paletou, F., Petit, P., Toqué, N., Alecian, E., Folsom, C. 2006, *A&A* 451, 293
- Woolf, V. M., Lambert, D. L. 1999, *ApJ* 521, 414
- Wright, G. A. E. 1973, *MNRAS* 162, 339

**Table 3.** Magnetic field measurements of possible cluster Ap stars

Star	HJD	SNR	$v_r$ (km s <sup>-1</sup> )	$\langle B_z \rangle \pm \sigma_B$ (G)	fld
HD 16605	2453570.110	608	-1	-2099 $\pm$ 34	DD
	2453571.081	689	-1	-2205 $\pm$ 29	DD
HD 16728	2453572.123	1510		-2 $\pm$ 272	
HD 19805	2453570.131	1045	0	6 $\pm$ 24	
	2453572.129	1453	0	-3 $\pm$ 14	
HD 108945	2453569.732	1884	+1	-111 $\pm$ 28	DD
	2453569.740	1872	+1	-75 $\pm$ 29	DD
	2453570.735	2487	+1	109 $\pm$ 20	DD
HD 144661	2453571.758	2814	-3	-55 $\pm$ 48	
	2453571.758	2946	-4	11 $\pm$ 48	
HD 153948	2453569.768	1005	-2	-222 $\pm$ 82	DD
	2453570.774	942	-2	-185 $\pm$ 89	DD
	2453571.778	901	-3	199 $\pm$ 90	
HD 317857	2453571.810	568	-10	-919 $\pm$ 20	DD
HD 318100	2453569.804	597	-8	-644 $\pm$ 59	DD
HD 162576	2453568.870	1861	-14	10 $\pm$ 25	DD
	2453569.828	1568	-13	-19 $\pm$ 28	
	2453570.797	2498	-13	13 $\pm$ 18	
HD 162588	2453568.884	1625	-16	93 $\pm$ 84	
	2453569.846	1039	-15	41 $\pm$ 141	
	2453571.858	2016	-13	36 $\pm$ 70	
HD 162630	2453570.819	1229	-15	-61 $\pm$ 117	
	2453571.872	1407	-13	-157 $\pm$ 116	
HD 162656	2453571.885	1338	+3	24 $\pm$ 78	
HD 162725	2453566.876	1654	-14	-101 $\pm$ 14	DD
	2453569.865	1608	-13	-21 $\pm$ 20	DD
HD 320764	2453568.858	1212		-399 $\pm$ 408	
	2453571.832	1131		137 $\pm$ 448	
HD 169842	2453566.902	1395	-30	180 $\pm$ 20	DD
	2453569.890	930	-30	230 $\pm$ 30	DD
	2453570.858	1441	-30	-153 $\pm$ 21	DD
HD 169959A	2453570.885	1378	-53	-691 $\pm$ 113	DD
HD 170054	2453569.925	781	-28	12 $\pm$ 108	
	2453570.888	1556	-26	-87 $\pm$ 54	
HD 170860	2453571.901	1005	-13	462 $\pm$ 236	DD
HD 172271	2453567.897	1441	-21	-265 $\pm$ 90	
HD 205073	2453567.914	1395	-7	4 $\pm$ 15	
	2453569.972	1102	+18	-8 $\pm$ 21	
HD 205331	2453567.922	1614	-5	-49 $\pm$ 41	
	2453570.003	2022	-4	-9 $\pm$ 33	
	2453570.967	1688	-3	143 $\pm$ 41	
BD +49-3789	2453570.941	528	-6	561 $\pm$ 400	
HIP 109911	2453570.033	545	-10	494 $\pm$ 230	

**Table 4.** Comparison of ESPaDOnS and FORS1 measurements of the same stars

Star	$m_V$	$T_{\text{eff}}$ (K)	$v_e \sin i$ (km s <sup>-1</sup> )	Instrument	HJD	$\Delta t$ (min)	SNR	$\langle B_z \rangle \pm \sigma_B$ (G)	fld
HD 108945	5.46	8800	65	FORS1		15	1250	$-44 \pm 75$	nnn
				ESPaDOnS	2453569.732	12	1880	$-111 \pm 28$	DD
				ESPaDOnS	2453569.740	12	1870	$-75 \pm 29$	DD
				ESPaDOnS	2453570.735	15	2490	$109 \pm 20$	DD
HD 153948	9.35	10600	80	FORS1		70	3100	$195 \pm 53$	DnD
				ESPaDOnS	2453569.768	40	1000	$-222 \pm 82$	DD
				ESPaDOnS	2453570.774	38	940	$-185 \pm 89$	DD
				ESPaDOnS	2453571.778	37	900	$199 \pm 90$	ND
HD 317857	10.30	10000:	26	FORS1		75	2150	$-1558 \pm 54$	DDD
				ESPaDOnS	2453571.810	46	570	$-919 \pm 20$	DD
HD 318100	9.84	10600	42	FORS1		47	2100	$345 \pm 64$	DnD
				ESPaDOnS	2453569.804	50	600	$-644 \pm 59$	DD
HD 162725	6.42	9600	32	FORS1		46	4450	$-60 \pm 33$	nnn
				ESPaDOnS	2453566.876	20	1650	$-101 \pm 14$	DD
				ESPaDOnS	2453569.865	26	1610	$-21 \pm 20$	DD
HD 320764	8.90	8500	225	FORS1		36	2400	$-69 \pm 66$	nnn
				ESPaDOnS	2453568.858	33	1212	$-399 \pm 408$	ND
				ESPaDOnS	2453571.832	38	1131	$137 \pm 448$	ND
HD 169959A	7.57	11000	57	FORS1		30	2550	$-486 \pm 52$	DnD
				ESPaDOnS	2453570.885	25	1378	$-691 \pm 113$	DD
HD 170054	8.18	14500	26	FORS1		42	2300	$64 \pm 68$	nnn
				FORS1		36	2200	$84 \pm 77$	nnn
				ESPaDOnS	2453569.925	52	780	$12 \pm 108$	ND
				ESPaDOnS	2453570.888	27	1560	$-87 \pm 54$	ND
HD 170860	9.39	13700	85	FORS1		45	2050	$-41 \pm 61$	nnn
				ESPaDOnS	2453571.901	43	1005	$462 \pm 236$	DD

**Table 5.** Physical properties of stars that are probable or certain open cluster members, probable or certain Ap stars, and have new ESPaDOnS magnetic field measurements.

Cluster	$\log t$ (yr)	true DM	Star	$\log T_e$ (K)	$\log L/L_\odot$	$M/M_\odot$	fractional age	$B_{\text{rms}}$ (G)	$n_B$
NGC 1039	$8.33 \pm 0.06$	8.49	HD 16605	4.025	1.65	$2.55 \pm 0.15$	$0.40 \pm 0.09$	1894	5
Coma Ber	$8.70 \pm 0.10$	4.70	HD 108945	3.944	1.60	$2.30 \pm 0.15$	$0.71 \pm 0.21$	93	4
NGC 6281	$8.45 \pm 0.10$	8.86	HD 153948	4.025	1.86	$2.70 \pm 0.15$	$0.62 \pm 0.18$	201	4
NGC 6405	$7.80 \pm 0.15$	8.44	HD 318100	4.025	1.64	$2.50 \pm 0.10$	$0.11 \pm 0.04$	517	2
NGC 6475	$8.41 \pm 0.05$	7.24	HD 162576	4.004	2.17	$3.10 \pm 0.15$	$0.81 \pm 0.17$	15	3
			HD 162588	4.033	2.10	$3.05 \pm 0.20$	$0.77 \pm 0.17$	34	3
			HD 162725	3.982	2.36	$3.30 \pm 0.20$	$0.94 \pm 0.20$	69	3
NGC 6633	$8.75 \pm 0.05$	7.93	HD 169842	3.924	1.62	$2.35 \pm 0.10$	$0.85 \pm 0.18$	315	8
IC 4725	$8.02 \pm 0.05$	10.44	HD 170860	4.137	2.63	$4.25 \pm 0.20$	$0.71 \pm 0.15$	40	1
IC 4756	$8.44 \pm 0.06$	7.59	HD 172271	4.013	1.98	$2.85 \pm 0.15$	$0.69 \pm 0.16$	265	1
NGC 7243	$8.06 \pm 0.10$	9.54	BD+49 3789	4.111	2.23	$3.55 \pm 0.15$	$0.51 \pm 0.15$	561	1
			HIP 109911	4.114	2.29	$3.65 \pm 0.15$	$0.54 \pm 0.16$	494	1